Los Alamos
NATIONAL LABORATORY

memorandum
Spallation Neutron Source Project Office

To/MS: Distribution
From/MS: Sergey Kurennoy / H824
Phone/FAX: 5-1459 / 5-9998
Email: kurennoy@lanl.gov
Symbol: SNS: 2000-011
Date: February 28, 1999

SUBJECT: Beam position monitors for SNS linac

Copies to:

SNS File	MS H824		
A.V. Aleksandrov	MS H808 (e-copy)	J.F. O'Hara	MS H808 (e-copy)
J.H. Billen	MS H824 (e-copy)	J.F. Power	MS H824 (e-copy)
J.D. Gilpatrick	MS H808 (e-copy)	R.E. Shafer	MS H808 (e-copy)
R.A. Hardekopf	MS H824 (e-copy)	J.E. Stovall	MS H824 (e-copy)
A.J. Jason	MS H808 (e-copy)	L.R. Doolittle	LBNL (e-copy)
R.B. Miller	MS H824 (e-copy)	P.R. Cameron	BNL (e-copy)
S. Nath	MS H824 (e-copy)	T.J. Shea	BNL (e-copy)

Abstract*. Electromagnetic modeling of various options for the SNS linac beam positions monitors (BPMs) has been performed to choose an optimal design. Results are presented and discussed.*

1. Introduction

Beam position monitors (BPMs) are a very important part of the linac beam diagnostics system. Information about the transverse position of the beam delivered by the BPMs is used to steer the beam properly in the linac with the steering magnets. In addition, using the summed signals from all the BPM electrodes provides a good way to measure accurately the beam phase, see [1].

Exact requirements on the resolution and accuracy, as well as the total number of the BPMs, depend on a particular choice of the beam steering scheme in the linac. Typical values for the accuracy are on the order of 0.1 mm in the beam position within, say, 1/3 of the bore radius r_b from the axis (r_b is between 1cm and 2 cm for the normal conducting SNS linac).

One specific feature of linac BPMs is their high signal processing frequency, which is usually equal to the repetition frequency f_b of microbunches in the linac (or one of its lowest harmonics). For the SNS linac f_b=402.5 MHz, much higher than typical revolution frequencies in rings. Another feature is a rather limited length along the beam line, which is available for the BPM transducer in ion linacs, especially at low beam energies. This imposes certain restrictions on the linac BPM design.

An option to use summed signals from the BPM electrodes for the linac beam-phase detection requires some extra signal power, but has an obvious advantage that no additional special devices on the beam line for phase measurements are required. On the other hand, the total number of BPMs will probably increase since the phase detectors have to be located at certain positions on the beam line, near the ends of RF modules.

To study and compare different options for the transducers of the SNS linac beam position monitors, we use the electromagnetic (EM) code package MAFIA [2]. Electrostatic 2-D computations are first used to adjust the BPM cross-section parameters to have 50-Ω transmission lines. After that 3-D static and time-domain computations are applied to calculate the electrode coupling. Time-domain 3-D simulations with an SNS beam microbunch passing through the corresponding beam-line device at a varying offset from the chamber axis have been performed to model the BPM response. The induced voltages on the electrodes are computed as functions of time. After that an FFT procedure is applied to extract the amplitudes and phases of the signal harmonics at individual outputs, as well as the amplitude and phase of the combined (summed) signal, versus the beam transverse position. We concentrate primarily on the first and second harmonics of the SNS bunch repetition frequency f_b=402.5 MHz as the most appropriate ones for the beam position and beam phase diagnostics.

2. Electromagnetic modeling of BPMs

To conform the restrictions mentioned above, it was decided to choose 4-electrode BPM design with one-end-shorted stripline electrodes. Such a design provides a rigid and robust mechanical structure with a good repeatability from one device to another, so that detailed mappings in the lab will be required for a few BPMs only. The design is bi-directional, which may be useful in tight spots. It also saves four connectors, and since the remaining four are all on one end of the BPM, the device can be mounted close to quadrupoles. The disadvantage of using the electrodes shorted at one end is the difficulty of their proper matching with a 50-Ω connector on the other end, compared to the stripline electrodes having 50-Ω connectors on both ends.

The signal power in a BPM transducer for a given beam current can be increased by increasing the length and width of the electrodes (lobes). Obviously, the electrode length is limited by available space on the beam line, in some cases as short as 2 inches. Wider electrodes generally provide a better linearity, but for very wide lobes the gap separating them is getting small, and one can expect a noticeable coupling. Within these constraints, we considered and numerically modeled a few possible designs.

Two MAFIA models for the BPM assembly consisting of a box with 4 electrodes on a beam pipe are shown in Fig. 1. The electrodes are flush with the beam pipe, shorted at one end, and have 50-Ω connectors on the other end (connectors are not shown in Fig. 1a). The beam pipe radius in the model is 20 mm, the electrode length along the beam is 40 mm, and their subtended angle is 60°. The 50-Ω terminations of the electrodes are modeled by filaments with discrete elements, 50-Ω resistors in this case.

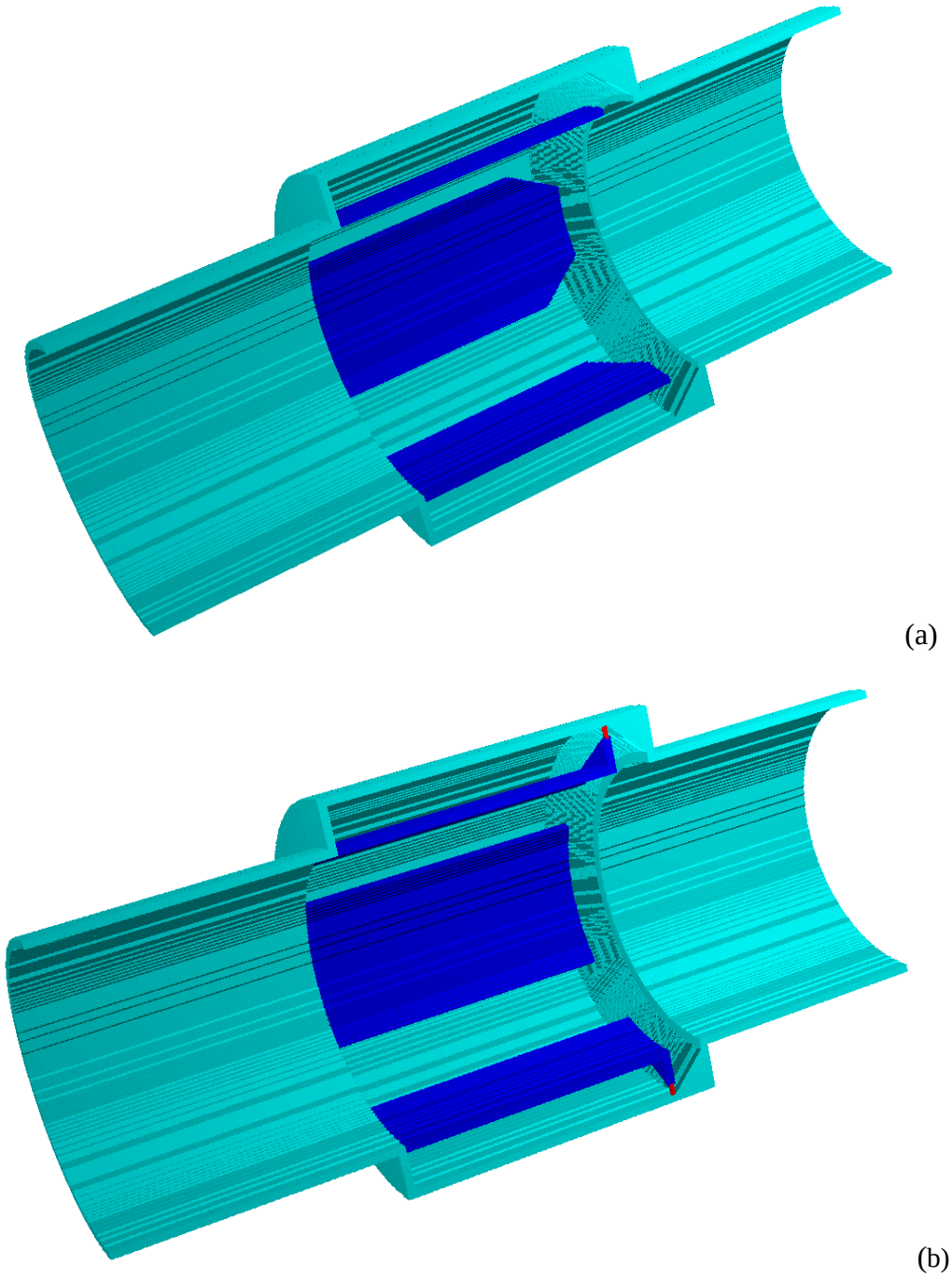

Figure 1: MAFIA models of SNS linac BPMs (one-half cutout) with cone-tapered box: (a) tapered electrodes (dark-blue) and (b) electrodes with modified terminations (connectors are shown in red).

The coupling between BPM electrodes was calculated in two different ways. In a static approximation we solve a 2-D electrostatic problem to find potentials on passive electrodes with a given potential on an active one. A similar procedure is used to adjust the BPM cross section for the electrodes to form 50-Ω transmission lines. In the dynamical 3-D problem, a 402.5-MHz *sin*-signal with the amplitude increasing to some level is fed into a connector of the active

electrode, and the induced signals on the passive ones are calculated. In both cases, the coupling coefficients are defined as ratios of the potentials or voltage amplitudes: $k_{12}=A_2/A_1$ for two adjacent electrodes, and $k_{13}=A_3/A_1$ for two opposite ones. Figure 2 illustrates the static coupling between the BPM electrodes for three different types of the BPM cross section. One can see, that inserting the separators – the metal ridges connected to the BPM box and filling the gap between the adjacent electrodes – reduces the static coupling to about half of that without them. With the separators inserted, the coupling of 60° electrodes (left) is reduced (center) to that of 45° electrodes (right).

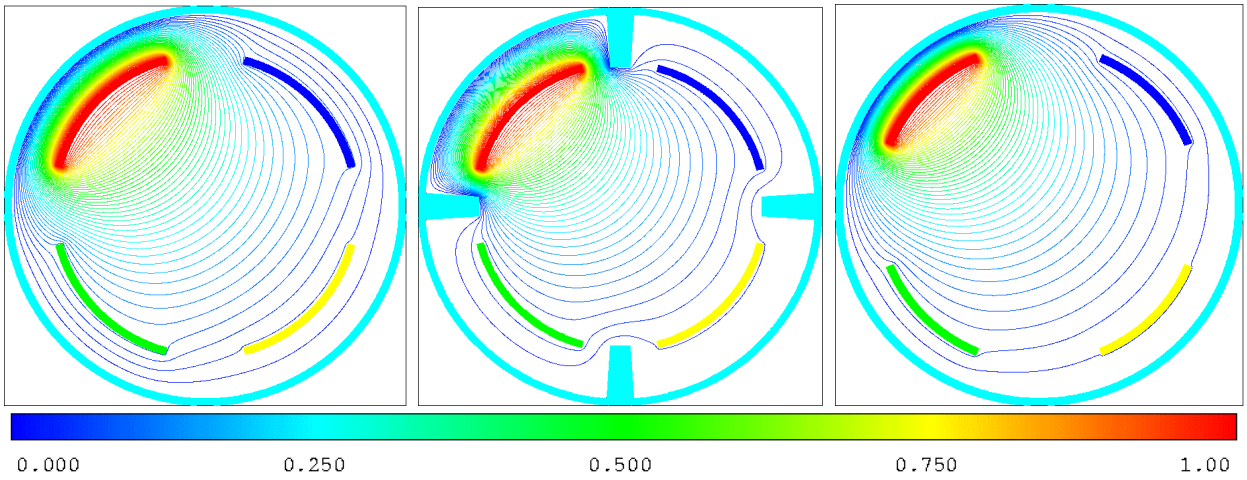

Figure 2: Electrostatic coupling in three BPMs: 60° electrodes (left), the same with separators (center), and 45° electrodes (right). The color of equipotential lines corresponds to the scale below.

Direct 3D time-domain computations with an ultra relativistic ($\beta=1$) bunch passing the structure at the axis or parallel to the axis have been performed for a few layouts of the BPM transducers. A Gaussian longitudinal charge distribution of the bunch with the total charge $Q=0.14$ nC and the rms length $\sigma=5$ mm, corresponding to the 56-mA current in the baseline SNS regime with 2-MW beam power at 60 Hz, was used in the simulations. Unfortunately, the MAFIA time-domain code T3 at present cannot simulate the open boundary conditions on the beam pipe ends for non ultra relativistic ($\beta<1$) beams. In the next section, the ultra relativistic MAFIA results are used to fix parameters of an analytical model for the BPMs at $\beta=1$, and then to derive results for $\beta<1$ analytically. For illustration, Fig. 3 shows the voltages on all four electrodes versus time for the case of a beam displaced from the chamber axis by $x=r_b/2$ (half aperture) horizontally and by $y=r_b/4$ vertically, and their corresponding Fourier transforms, for the BPM of Fig. 1b. Indices *R,T,L,B* here refer to the right, top, left and bottom electrodes of the BPM. The Fourier spectra of the signals have first peaks near 2 GHz, that corresponds approximately to the wavelength $\lambda/4=l$.

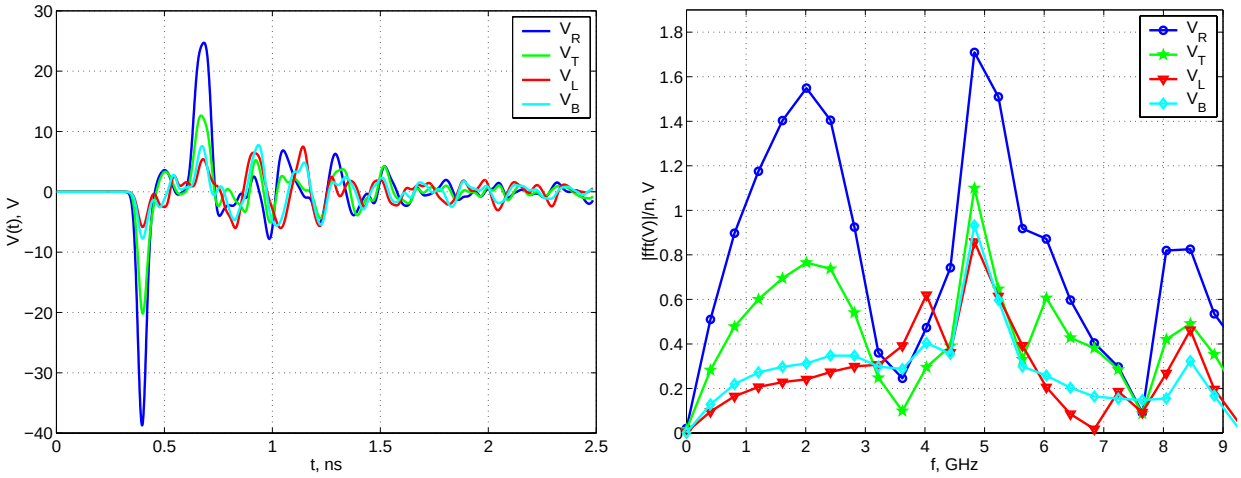

Figure 2: Signals on four BPM electrodes from a passing transversely displaced ($x=r_b/2$, $y=r_b/4$) bunch: left – voltages versus time during one period $T=1/f_b=2.4845$ ns; right – normalized Fourier transform amplitudes (V) versus frequency.

Table 1 summarizes our simulation results for a few different BPM types. It lists the static and dynamic couplings, the maximal signal voltage on the electrodes from the on-axis beam, the amplitude and corresponding signal power of the 1st Fourier harmonic (at 402.5 MHz).

Table 1: Comparison of different designs for 4-electrode SNS BPM (with on-axis beam).

BPM type			**Calculation results**				
electrode shape	angle, °	length, mm	$k_{st\ 12}$, %; $k_{st\ 13}$, %	$k_{dyn\ 12}$, %; $k_{dyn\ 13}$, %	$\|V(t)\|_{max}$, V	$\tilde{A}_1$, V	P, dBm
rectangular	45	26	0.13; 0.05	1.8; 0.55	13.5	0.118	-8.5
rectangular	60	26	0.21; 0.09	2.6; 0.74	14	0.155	-6.2
rect., with separators	60	26	0.13; 0.05	1.1; 0.34	10	0.120	-8.4
2 50-Ω terminations	60	26	0.21; 0.09	1.4; 0.5	13	0.150	-6.5
rectangular	60	40	0.34; 0.15	3.6; 1.1	12.5	0.189	-4.5
tapered	60	40	same	3.6; 1.1	13.9	0.245	-2.2
tapered, cone box*	60	40	same	3.7; 1.2	14	0.244	-2.3
tapered, cone, separ.	60	40	0.13; 0.05	1.7; 0.57	11.5	0.161	-5.9
cone box, mod. term.*	60	40	0.34; 0.15	5.1; 1.6	18	0.255	-1.9

The cases marked by the star in Table 1 are those shown in Fig. 1. One can see from this summary that introducing the separators reduces the electrode coupling but at the same time the signal power decreases. Having two 50-Ω connectors on both ends of the electrode also reduces the dynamical coupling, with about the same signal power as in the one-end-shorted design. However, such a design is more complicated and more expensive, as well as less reliable mechanically, compared to the one-end-shorted version. To study the BPM linearity, we perform simulations with the beam bunch passing through the BPM at different transverse positions. The results for the BPM design with modified terminations (Fig. 1b) are presented in Table 2.

Table 2: Amplitudes of signal harmonics on 4 electrodes of 60° BPM for a few beam transverse positions.

Beam position		@ 402.5 MHz		@ 805 MHz	
x/r	y/r	$\tilde{A}_R$ $\tilde{A}_T$ $\tilde{A}_L$ $\tilde{A}_B$, V	$\tilde{A}_\Sigma$, V	$\tilde{A}_R$ $\tilde{A}_T$ $\tilde{A}_L$ $\tilde{A}_B$, V	$\tilde{A}_\Sigma$, V
0	0	0.255	1.021	0.44	1.76
0.25	0	0.374 0.240 0.168 0.240	1.022	0.65 0.41 0.29 0.41	1.76
0.25	0.125	0.368 0.291 0.166 0.196	1.021	0.64 0.50 0.28 0.34	1.76
0.25	0.25	0.351 0.352 0.158 0.158	1.018	0.608 0.610 0.270 0.271	1.76
0.5	0	0.540 0.194 0.103 0.194	1.031	0.95 0.33 0.18 0.33	1.78
0.5	0.125	0.533 0.235 0.101 0.159	1.027	0.94 0.40 0.17 0.27	1.78
0.5	0.25	0.510 0.282 0.096 0.129	1.016	0.90 0.48 0.16 0.22	1.75
0.5	0.375	0.469 0.339 0.088 0.101	0.997	0.82 0.58 0.15 0.17	1.72
0.5	0.5	0.408 0.409 0.077 0.077	0.970	0.702 0.704 0.135 0.135	1.67

As one can see from this table, at high beam energies the signal power at 402.5 MHz changes from its maximal value of +4.6 dBm to the minimal one –12.3 dBm at the beam position changes within a rather wide range, $\{x,y\in(-r_b/2,r_b/2)\}$. This corresponds to the signal dynamical range of 16.9 dB.

The BPM linearity results derived from this kind of data are presented in Figs. 4-5. Figure 4 shows the horizontal signal processing ratio – the log ratio $\ln(\tilde{A}_R/\tilde{A}_L)/2$ or the difference-over-sum ratio $S=(\tilde{A}_R-\tilde{A}_L)/(\tilde{A}_R+\tilde{A}_L)$ – versus the beam horizontal displacement x/r_b, for a few values of the beam vertical displacement y/r_b. The results for different vertical beam positions overlap, so that is difficult to distinguish between the five interpolating lines. Therefore, this BPM design is very insensitive to the beam position in the direction orthogonal to the measured one. Another way to look at this is presented in Figure 5, where the contours of equal log ratios are projected onto x,y-plane. Small visible distortions of these contours are observed only outside

the region of about 1/3 of the aperture. From these results, one can conclude that the BPM design with 60° electrodes and the modified transitions (Fig. 1b) has a very good linearity. We have also found that the linearity of BPMs with separators is much worse, in spite of the lower coupling.

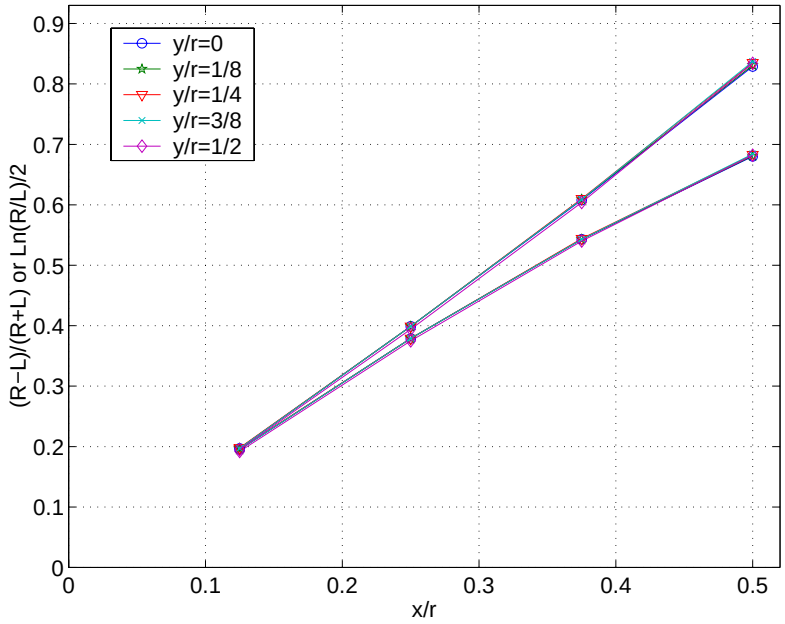

Figure 4: MAFIA results for horizontal ratio S of the signal harmonics at 402.5 MHz (top lines for $S=\ln(\tilde{A}_R/\tilde{A}_L)/2$, bottom ones for $S=(\tilde{A}_R-\tilde{A}_L)/(\tilde{A}_R+\tilde{A}_L)$) versus the beam horizontal displacement x/r_b, for a few values of the beam vertical displacement y/r_b (see legend).

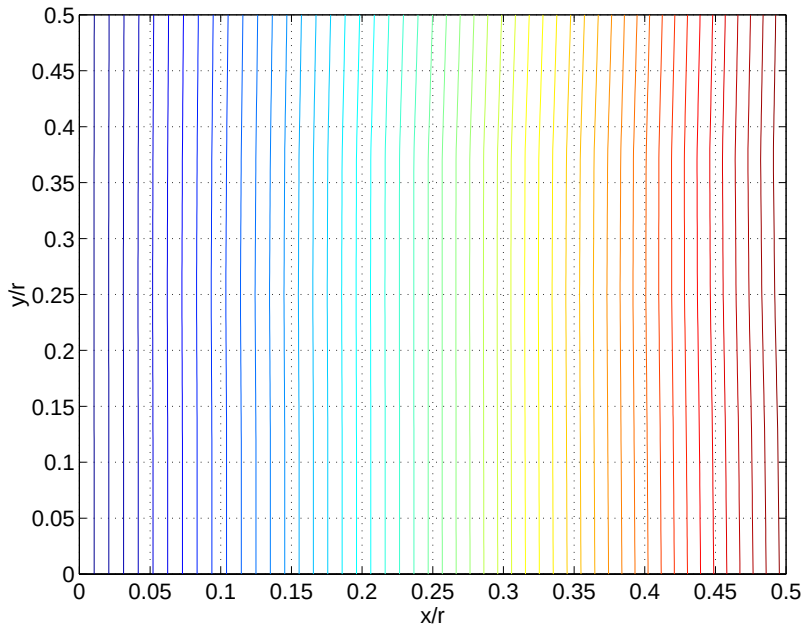

Figure 5: Contours of equal ratio $S=\ln(\tilde{A}_R/\tilde{A}_L)/2$ for signal harmonics 402.5 MHz (MAFIA results).

3. Analytical model of BPM

If one assumes an approximate axial symmetry of the beam pipe, the signals on the BPM electrodes with inner radius r_b and subtended angle φ can be calculated by integrating induced currents within the electrode angular extent. For a pencil beam bunch passing the BPM at the transverse position $x=r\cos\theta$, $y=r\sin\theta$ at velocity $v=\beta c$, the signals are (e.g., [3])

$$R(f,r,\theta) = C\,\frac{\varphi}{2\pi}\left[\frac{I_0(gr)}{I_0(gr_b)} + \frac{4}{\varphi}\sum_{m=1}^{\infty}\frac{I_m(gr)}{I_m(gr_b)}\sin\left(m\phi/2\right)\cos\left(m\theta\right)\right], \tag{1}$$

$$T(f,r,\theta) = C\,\frac{\varphi}{2\pi}\left[\frac{I_0(gr)}{I_0(gr_b)} + \frac{4}{\varphi}\sum_{m=1}^{\infty}\frac{I_m(gr)}{I_m(gr_b)}\sin\left(m\phi/2\right)\cos\left(m\left(\theta-\pi/2\right)\right)\right], \tag{2}$$

$$L(f,r,\theta) = C\,\frac{\varphi}{2\pi}\left[\frac{I_0(gr)}{I_0(gr_b)} + \frac{4}{\varphi}\sum_{m=1}^{\infty}\frac{I_m(gr)}{I_m(gr_b)}\sin\left(m\left(\pi+\phi/2\right)\right)\cos\left(m\theta\right)\right], \tag{3}$$

$$B(f,r,\theta) = C\,\frac{\varphi}{2\pi}\left[\frac{I_0(gr)}{I_0(gr_b)} + \frac{4}{\varphi}\sum_{m=1}^{\infty}\frac{I_m(gr)}{I_m(gr_b)}\sin\left(m\left(\pi+\phi/2\right)\right)\cos\left(m\left(\theta-\pi/2\right)\right)\right], \tag{4}$$

where R,T,L,B are the Fourier components at frequency f of the signals on the right, top, left, and bottom electrodes of the BPM, correspondingly. Here $I_m(z)$ are the modified Bessel functions of the first kind, all dependence on frequency and energy enters through the geometrical coefficient $g=2\pi f/(\beta\gamma c)$, and overall coefficient C depends on the bunch current and shape.

The geometrical parameters of the BPM cross-section, r_b and φ, can be considered as "free" parameters of the model. Obviously, the induced current on an electrode in the real geometry is larger than an integral of the current density over the angle φ in an axisymmetric pipe of radius r_b, since more electric field lines from the passing bunch ends up on the electrode compared to the circular pipe segment of the same radius and angular extent. We will use Eqs. (1)-(4) to fit our MAFIA computation results for $\beta=1$, and to fix effective values of r_b and φ. One can expect these effective values to be larger than geometrical ones.

One can introduce the coupling between the electrodes in our model to make it more realistic. If k_{12} denotes the coupling coefficient between adjacent electrodes, and k_{13} between the opposite ones, the coupled signals (1)-(4) can be written as

$$R_c = \left[R + k_{12}\left(T+B\right) + k_{13}L\right]/\left(1+2k_{12}+k_{13}\right) \quad , \tag{5}$$

and similar for T_c,L_c,B_c, via cyclic permutations of R,T,L,B.

The fits of the numerical results at 402.5 MHz for the ratio $S/(x/r_b)$, where S is either the log ratio $\ln(\tilde{A}_R/\tilde{A}_L)/2$ or the difference-over-sum ratio $(\tilde{A}_R-\tilde{A}_L)/(\tilde{A}_R+\tilde{A}_L)$, with our model are shown in Fig. 6. The MAFIA data are represented by the points colored according to the beam vertical displacement y/r_b that changes from 0 to 1/2 in steps of 1/8. The computed values of S for different y/r_b are close to each other, especially for small vertical deflections (cf. Fig. 4). This causes the data points to overlap in the picture, and in many cases only the color of the last

plotted point is observed. The best fit to the numerical data, represented by colored curves in Fig. 6, was obtained with the effective parameters r_{eff}=1.17r_b, φ_{eff}=1.24φ (=74.5°), and k_{12}=k_{13}=0, where r_b=20 mm, φ=π/3 rad are the geometrical values. It is interesting to note that the effective radius r_{eff}=23.4 mm is close to the average of the electrode inner radius r_b=20 mm and that of the BPM box, 26.5 mm, in agreement with earlier observations [4].

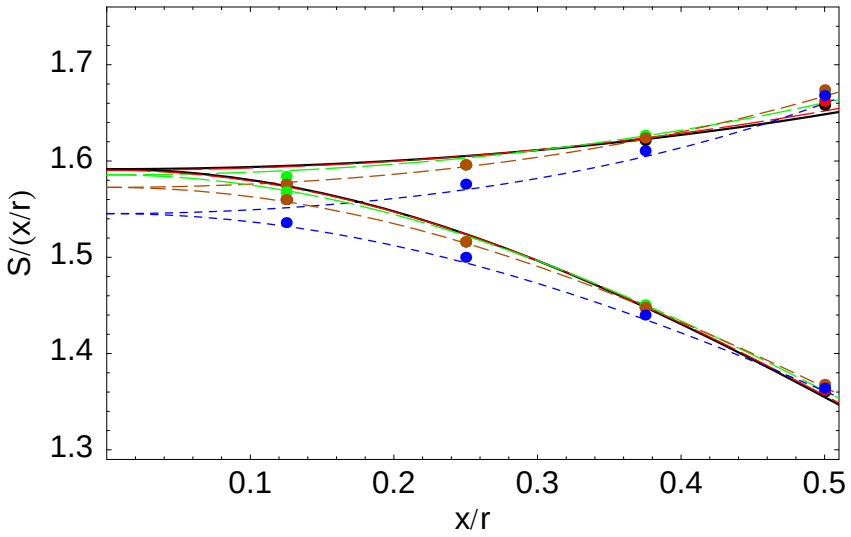

Figure 6: Fitting MAFIA results (dots) for $S/(x/r_b)$ at 402.5 MHz with the analytical model (top lines for $S=\ln(\tilde{A}_R/\tilde{A}_L)/2$, bottom ones for $S=(\tilde{A}_R-\tilde{A}_L)/(\tilde{A}_R+\tilde{A}_L)$). Color of curves and dots corresponds to the beam vertical displacement: y/r_b= 0 – black, 1/8 – red, 1/4 – green, 3/8 – brown, 1/2 – blue.

Attempts to introduce a non-zero coupling, even as small as 1%, lead to a rather wide spread between the curves for different y/r_b, so we have to conclude that the numerical results strongly suggest very small coupling between the BPM electrodes. It seems to be in contradiction with the dynamical coupling coefficients presented in Table 1. One can think, however, that the azimuthal modes providing the electrode coupling when the 402.5-MHz signal is fed into one of the connectors, are not excited by the passing beam.

Matching the amplitude of 402.5-MHz harmonics from an on-axis ultra relativistic SNS beam bunch with Eqs. (1)-(4) fixes the overall constant C=1.232. The 402.5-MHz signal amplitudes for the displaced beams in Table 2 are then reproduced by the model with the accuracy 1-2%. Assuming that the derived effective parameters of the model are applicable also at lower beam velocities, we extrapolate our β=1 results for β<1. The signal power versus the beam velocity is shown in Fig. 7 for two different transverse beam positions. The power level for the on-axis beam is reduces by about 9 dB at β=0.073 (2.5 MeV). For the strongest signal in the beam displacement range (-r_b/2, r_b/2) both vertically and horizontally, this reduction is 4.4 dB, and for the weakest one is 12.9 dB. As a result, the dynamical range of the 402.5-MHz signal shifts from about 17 dB for β=1 to about 25 dB at β=0.073, if the same radius of BPM is assumed. Of course, at the low-energy end the bore radius is smaller, so that the power level will

be higher. Figures 7 illustrate the signal power change with the beam energy for a given BPM radius.

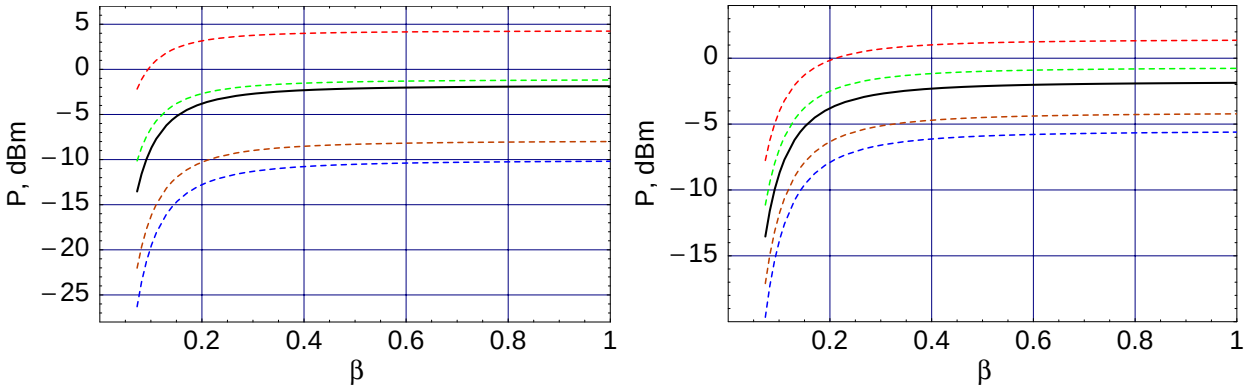

Figure 7: Power of 402.5-MHz signals on four BPM electrodes versus the beam velocity for two beam transverse positions: $x/r_b=1/2$, $y/r_b=1/4$ (left) and $x/r_b=1/4$, $y/r_b=1/8$ (right) – colored dashed curves, and for the same beam on axis – black solid line.

4. BPMs as phase probes

The application of the linac BPMs as the beam-phase probes and their favorable comparison with the capacitive probes has been studied earlier [1]. Here we present some results on the beam phase for the particular BPM design with 60° electrodes and the modified terminations (Fig. 1b).

For each beam displacement, the phases of the voltage Fourier transforms, as well as the amplitude and phase of the summed signal, have been recorded. The results for the fundamental harmonic f_b=402.5 MHz and the second one, 805 MHz, are summarized in Table 3. Since we are mostly interested in the phase difference between the signals from an on-axis and off-axis beams, the beam phase of the centered beam (-170.09° at 402.5 MHz and 114.80° at 805 MHz) was subtracted from the phases in the table. For the computations in our MAFIA model a relatively crude mesh with a step d=0.5 mm in all three dimensions has been used, that resulted in about 3 millions mesh points. Therefore, one can roughly estimate the accuracy of all calculated phases as corresponding to the time interval $\Delta t=d/2/c$=0.83 ps, where c is the speed of light. If one takes the time interval between bunches $T=1/f_b$=2.4845 ns to be 360°, then $\pm\Delta t$ corresponds to ±0.12° for 402.5 MHz, and twice that at 805 MHz. The signal phases on individual electrodes differ by a few degrees, while the phases of the summed signals are equal, within this accuracy interval, for all beam displacements. The only exception is possibly the case of a rather strong offset $x=r_b/2$, $y=r_b/2$ at 805 MHz (the last line in the table, highlighted by yellow). However, even in this last case the calculated deviation is only about 0.6°, which could be just as well a numerical effect, and it is certainly very small compared to the phase difference for the individual electrodes that spans about 17° in this case. The behavior of the signal phases versus the beam vertical position is shown in Figs. 8 for two particular horizontal deflections of the beam.

Table 3: Phases of signal harmonics for 4-electrode 60-degree SNS BPM for a few beam transverse positions.

Beam position		@ 402.5 MHz		@ 805 MHz	
X/r	y/r	ϕ_R ϕ_T ϕ_L ϕ_B,°	ϕ_Σ,°	ϕ_R ϕ_T ϕ_L ϕ_B,°	ϕ_Σ,°
0	0	0	0	0	0
0.25	0	0.94 -0.39 -1.25 -0.39	-0.04	1.90 -0.62 -3.01 -0.62	-0.08
0.25	0.125	0.89 0.14 -1.34 -0.98	-0.04	1.86 0.61 -3.22 -2.09	-0.06
0.25	0.25	0.71 0.64 -1.66 -1.63	-0.04	1.73 1.61 -3.90 -3.85	-0.04
0.5	0	1.68 -1.67 -2.85 -1.67	-0.03	2.96 -2.73 -7.57 -2.73	-0.18
0.5	0.125	1.65 -1.00 -2.97 -2.39	-0.03	2.99 -0.86 -7.85 -4.99	-0.13
0.5	0.25	1.57 -0.35 -3.35 -3.18	-0.03	3.06 0.76 -8.77 -7.52	0.01
0.5	0.375	1.39 0.30 -4.06 -4.09	-0.02	3.19 2.13 -10.55 -10.37	0.26
0.5	0.5	1.02 0.95 -5.23 -5.18	0.00	3.36 3.23 -13.72 -13.60	0.59

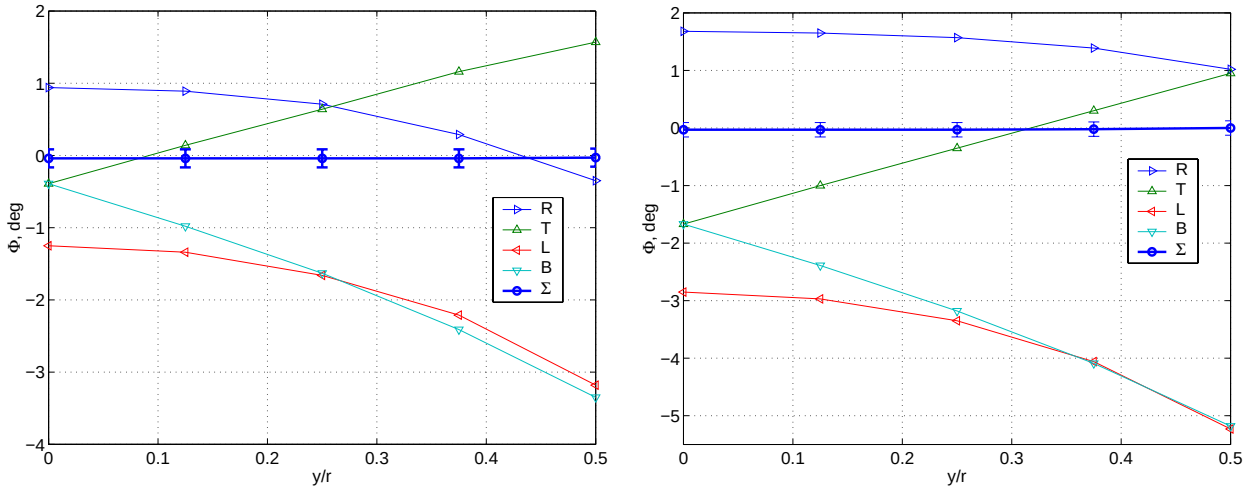

Figure 8: 402.5-MHz signal phases on four BPM electrodes and for the summed signal versus the beam vertical displacement y/r_b, for the beam horizontal displacement x/r_b=1/4 (left) and x/r_b=1/2 (right).

As one can see in Figs. 8, the signal phases on both horizontal electrodes behave similarly, but in the vertical plane the phase changes have opposite signs as the beam changes its vertical position. At the same time, the phase of the summed signal remains equal to that of the

on-axis beam, well within the computational errors (the error bars are shown only for the summed signal in Figs. 8). One should recall that we have modeled numerically only the $\beta=1$ case here, so that the beam fields reach the individual electrodes simultaneously independent of the beam transverse position, see the pictures of $V(t)$ in Figs. 3. However, the azimuthal modes in the BPM box are excited with different phases dependent on the beam position in the BPM transverse cross section, and this defines the phase differences between the electrodes.

5. Conclusions

The electromagnetic modeling of the linac BPMs has been performed with the MAFIA code package. Based on the results of this analysis, an optimal BPM design has been chosen. According to our simulations, it provides a very good linearity and sufficient signal power, while satisfying the linac geometrical limitations. The prototype of this BPM has just been manufactured, and it will be measured soon [5].

MAFIA time-domain simulations with the beam have been performed for the ultra relativistic ($\beta=1$) case; their results are presented in Sect. 2. In Sect. 3, these results are used as an input to an analytical model of the BPMs, and then some results for $\beta<1$ are derived analytically. The signal power decreases at 2.5 MeV by about 9 dB compared to 1 GeV for the on-axis beam. For the nominal 56-mA current in the beam displacement range $\{-r_b/2<x,y<r_b/2\}$, and for a fixed BPM radius $r_b=20$ mm, the dynamical range of the 402.5-MHz signal is from -25 dBm to 0 dBm at 2.5 MeV, cf. Figs. 7. This level is still comfortable for the signal processing, and it allows us to split the signal power from the BPM electrodes for combined measurements of the beam position and the beam phase while keeping the signal-to-noise ratio reasonable.

In Sect. 4 the simulation results for the signal phases are presented. In agreement with our previous study [1], for the BPMs, as well as for the capacitive probes, summing the signals from all connectors is required to measure the beam phase accurately. For an off-axis beam, the signal phases from individual electrodes can differ from those for a centered beam by a few degrees, cf. Table 3 and Figs. 8. The phase of a summed signal is rather insensitive to the beam transverse position inside the device and remains unchanged within the computation errors (0.1-0.2°) even for the beam offsets as large as the pipe half-aperture. Making the cable lengths from the electrodes to a summator to be equal with the corresponding accuracy (below 0.3 mm, or 1 ps) can be challenging, however, and might influence the BPM system configuration choice.

References

1. S.S. Kurennoy, “On Beam Phase Detectors for SNS Linac”, tech memo SNS: 99-65 (11/17/99).
2. MAFIA Release 4.20, CST GmbH, Darmstadt, 1999.
3. R.E. Shafer, in AIP Conf. Proceed. 319, 1993. – p.303.
4. R.E. Shafer, Private communication, 1999.
5. J.F. O’Hara, J.F. Power, Private communications, February 2000.